Chiral induction in thioester and oxoester liquid crystals by dispersed carbon nanotubes

Rajratan Basu [a] , Charles Rosenblatt [a] & Robert P. Lemieux [b]

[a] Department of Physics, Case Western Reserve University, Cleveland, Ohio, USA

[b] Department of Chemistry, Queen's University, Kingston, Ontario, Canada

PLEASE SCROLL DOWN FOR ARTICLE

Taylor & Francis
Taylor & Francis Group

Chiral induction in thioester and oxoester liquid crystals by dispersed carbon nanotubes

Rajratan Basu[a], Charles Rosenblatt[a]* and Robert P. Lemieux[b]

[a]*Department of Physics, Case Western Reserve University, Cleveland, Ohio, USA;* [b]*Department of Chemistry, Queen's University, Kingston, Ontario, Canada*

Multi-walled carbon nanotubes were dispersed at low concentrations into various achiral liquid crystals having either a thioester or oxoester linkage group in the core. The presence of the carbon nanotubes resulted in chiral signatures being observed in the liquid crystals, including an electroclinic effect (a rotation of the liquid crystal director perpendicular to, and linear in, an applied electric field) in both the nematic and smectic A phases, and a macroscopic helical twist of the liquid crystal director in the nematic phase. For both experiments the chiral signatures for the thioester liquid crystals were found to be an order of magnitude larger than those of the oxoesters. We speculate that the much larger strength of the thioester's chiral properties is a result of stronger non-covalent interactions between the liquid crystal molecule and carbon nanotube.

Keywords: chiral induction; ester; carbon nanotube; twist; electroclinic

1. Introduction

In liquid crystal (LC) phases the effect of a non-mesogenic guest (dopant) on the bulk properties of a LC host often depends on molecular recognition in order to process and propagate the 'information' coded into the structure of the dopant. One of the most common uses of dopants in liquid crystalline phases formed by calamitic molecules is the induction of chiral bulk properties, such as the helical pitch of a chiral nematic phase (N*), the electroclinic effect (ECE) of the chiral smectic A (SmA*) phase or the spontaneous polarisation of a chiral smectic C phase (SmC*) [1–5]. The physical interactions between LCs and carbon nanotube (CNT) dopants, due mainly to surface anchoring for $\pi - \pi$ electron stacking in a LC+CNT colloidal dispersion [6, 7], have drawn a great deal of interest in recent years [8–12]. These mixtures manifest a variety of fascinating phenomena, such as the interaction between the CNT-long axis and the LC director, improvement of the electrooptic response of the LCs, an electromechanical memory effect, and incremental changes in the LC orientational order parameter [8, 9, 13–15]. Recently, we used the ECE to demonstrate experimentally that multi-walled CNTs with a small enantiomeric excess transmit their inherent surface chirality to the nearby LC molecules [16, 17]; this induction of chirality also results in a helical macroscopic twist in a nematic matrix [18]. It is the extreme sensitivity to the CNTs' chirality using these techniques that facilitates our observation of even a small enantiomeric excess of CNTs. In this work we examine the CNTs' transmission of chirality into LCs possessing thioesters and oxoesters linking moieties.

In order to examine the chiral induction of the CNTs in the two types of mesogens – thioesters and oxoesters – we employed two experimental techniques: the ECE and a measurement of the induced helical pitch of the director. Garoff and Meyer [19] demonstrated an ECE in a bulk chiral SmA* LC phase, whereby an electric field $\vec{E}$ applied parallel to the smectic layer induces a polar tilt θ [$\propto E$] of the director in a plane perpendicular to $\vec{E}$. The tilt susceptibility $d\theta/dE$, also known as the electroclinic coefficient e_c, is temperature dependent and diverges on cooling toward the chiral SmC* phase transition temperature. The ECE involves the reduced C_2 symmetry of the lower temperature SmC* phase and is absent when the system is achiral or racemic. More recently it was shown that an ECE can occur in a chiral nematic phase as well [20–22], both in the bulk due to the presence of SmC-like fluctuations within the nematic phase [22] and at a surface, when an achiral LC is in contact with a chiral surface, even in the absence of smectic layer fluctuations [24, 25]. As does the ECE in the SmA* phase, both types of nematic electroclinic effects (NECEs) require the breaking of mirror symmetry. Previously we showed [16] that the thiophenyl benzoate LC $\overline{8}S5$ (Figure 1), when doped with multi-walled CNTs having a non-zero enantiomer excess (ee), exhibits an ECE in both the nematic and SmA phases due to the chirality induced in the LC by the nanotubes. The magnitude of e_c, which for the CNT

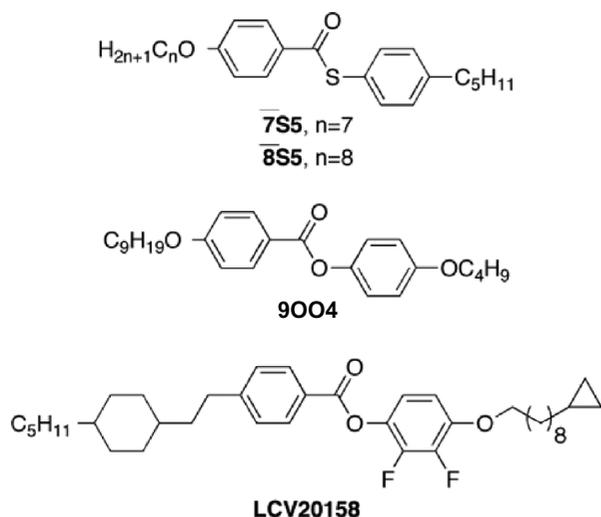*Corresponding author. Email: rosenblatt@case.edu

Figure 1. Liquid crystal mesogens used in this work.

dispersion corresponds to a spatially averaged tilt susceptibility $d\theta/dE$ owing to the relatively short range of the chiral induction [26], provides a measure of the 'chiral strength' of the CNT-induced chirality in an otherwise achiral LC. In this work we report on ECE measurements for both thiophenyl benzoate and phenyl benzoate mesogens doped with the same CNTs in order to obtain one metric for the relative chiral strength induced in the two types of moieties.

A second metric of chiral induction is the induced helical pitch P in the nematic phase. In an achiral nematic there is no ground state twist of the director, and thus the inverse pitch $P^{-1} = 0$; in a chiral nematic $P^{-1} \neq 0$, with increasing 'chiral strength' corresponding to increasing inverse pitch. Previously we showed that multi-walled CNTs having an enantiomer excess $ee \neq 0$ give rise to a chiral twist when mixed in an otherwise achiral nematic LC [18]. The pitch was very long, in some cases of the order of millimetres. Nevertheless, the pitch was measurable using the method of Raynes [27], and P^{-1} was found to be approximately linear in CNT weight fraction C_w, at least for C_w less than 0.0015–0.002. The idea behind Raynes' technique is that a 90° nematic twist cell with randomly scattered spacer beads, which are used to control the cell thickness, is filled with a LC, with or without a chiral dopant. If no chiral dopant is present and the LC is achiral, the director undergoes an approximately 90° twist from one substrate to the other, where the twist domains can be right- or left-handed and are separated by straight domain walls running between spacer beads. If a chiral dopant is present, the size of the surface-controlled 90° twist domain having the same handedness as the natural twist of the LC/dopant mixtures grows at the expense of the opposite-handed domains, and as a result the

domain walls become bowed. The radius of curvature of the domain walls is proportional to P. This approach facilitates measurements of pitch as large as tens of millimetres, and allows us to obtain a second metric for the relative strength of chiral induction by CNTs in thioester and oxoester LCs.

The chemical structures of the four LCs used in this experiment are shown in Figure 1. The phase sequence for $\overline{7}S5$ is Iso – 82° – N – 36° – SmC – 23° – Cryst; for $\overline{8}S5$ the phase sequence is Iso – 86° – N – 64° – SmA – 56° – SmC – 30.6° – SmJ – 14.6° – Cryst; for 9OO4 the phase sequence is Iso – 87° – N – 73° – SmA – 62° – SmC – 50° – SmB – 35° – Cryst; and for LCV20158 the phase sequence is Iso – 105° – N – 89° – SmA – 66° – SmC – 45° – Cryst. Note that the thiophenyl benzoates $\overline{7}S5$ and $\overline{8}S5$ contain a thioester linkage between aromatic groups, whereas the phenyl benzoates 9OO4 and LCV20158 contain an oxoester linkage.

2.   Experimental details

The multi-walled CNTs were obtained from Nanostructured & Amorphous Materials, Inc. and had an outer diameter of 8–15 nm, an inner diameter of 3–5 nm, length of 500–2000 nm and a distribution of different chiral strengths [18]. To reduce aggregation, a small number of CNTs were first dispersed in acetone and shaken on a vortex mixer for 15 min, followed by sonication for 2 h. LCs were then added to an appropriate amount of acetone + CNT mixture to achieve the desired final weight fraction C_w of CNTs in LC, and the mixture was sonicated for 1 h to facilitate complete dispersion. Finally, the acetone was evaporated at an elevated temperature, leaving a nearly pure LC–CNT mixture with the desired concentration C_w of CNTs. This process was repeated to prepare all of the LC–CNT mixtures. Although we attempted to use an identical CNT concentration in each mixture for the ECE measurements, there was a small but unavoidable variation from sample to sample. Thus $C_w = 0.002$ for $\overline{8}S5$, 0.0021 for $\overline{7}S5$, 0.0021 for LCV20158 and 0.0019 for 9OO4. For the pitch measurements we used $C_w = 0.0019$ for $\overline{7}S5$ and 0.0023 for 9OO4. We note that in the previous works [16–18] and in the study reported herein we took great care to confirm that the chiral signatures were not due to an artefact or chiral impurities. Indeed, we since have examined multi-walled CNTs from four different commercial sources, observing chiral signatures and thus a net enantiomeric excess – different for each manufacturer – in all batches of CNTs.

For the ECE measurements we used commercial cells from Instec Research Instrumentation Technology (LC3-05.0, planar rubbed, 5 mm × 5 mm semitransparent indium tin oxide (ITO) coated area

and a $d = 5$ μm spacing). The cells were filled by capillary action with the individual mixtures at temperatures in their respective isotropic phases. Note that the small cell spacing tends to filter out any nanotube aggregates larger than d. Based on previous measurements [18] of induced helical pitch in the nematic phase of the LC pentyl cyanobiphenyl, significant aggregation, that is, sufficient to begin causing deviations from linearity of the inverse pitch P^{-1} versus C_w, does not set in until $C_w \sim 0.002$. The experiments reported herein were performed at concentrations in this region. Before performing the ECE measurements, the LC–CNT cells were examined using a polarising optical microscope, which revealed uniform nematic, SmA and SmC textures (with phases appropriate to each LC) like those of a pure LC cell in the absence of CNTs, thus indicating a uniform director field. There was no indication of phase separation or agglomerates at any temperature. Thus, at least on visible light length scales, CNT-aggregates (if any) must be small enough to not perturb the director field due to their low concentration.

The optical setup for the ECE experiments consisted of a beam from a 5-mW He-Ne laser at wavelength 633 nm passing through a polariser, the cell, a crossed analyser and into a detector. The light's polarisation orientation was at an angle of $\pi/8$ with respect to the LC's director orientation; this is the 'classical' electroclinic geometry [28]. The output of the detector, proportional to the optical intensity at the detector, was fed into both a direct current (dc) voltmeter and a lock-in amplifier that was referenced to the driving frequency f of the ac electric field applied across the LC. Thus both the ac intensity I_{ac} at frequency f and the dc intensity I_{dc} were computer recorded as the applied ac field E was ramped upward with time over 500 s. From the resulting data in both the nematic and SmA phases we obtained the field-induced, spatially averaged director tilt angle θ using the formula $\theta = I_{ac}/4I_{dc}$ [28], which is plotted in Figure 2.

To measure the induced chiral twist, the LC cells were prepared using a pair of glass substrates that were spin-coated with the polyamic acid RN-1175 (Nissan Chemical Industries), baked and rubbed unidirectionally using a cloth-covered rubbing wheel. The two substrates were then placed together, separated by randomly dispersed spacer particles 10 μm in size, such that their rubbing directions were orientated at 90° with respect to each other [27]. Polarising microscope images were made of the $\overline{7}$S5 + CNT sample and the 9OO4 + CNT sample in their respective nematic phases, approximately 5°C below the isotropic–nematic transition temperature T_{NI}; the results are shown in Figure 3.
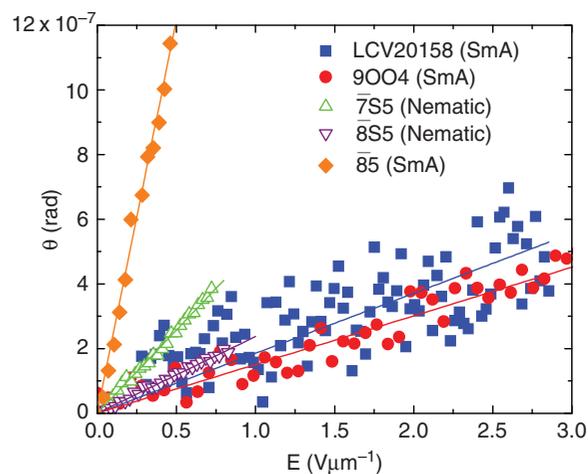

Figure 2. Induced tilt angle θ versus applied electric field E, such that the electroclinic coefficient $e_c \equiv d\theta/dE$. Solid lines are linear fits to the data. The solid blue square corresponds to LCV20185 in the SmA phase; solid red circles to 9OO4 in the SmA phase; open green upward triangle to $\overline{7}$S5 in the nematic phase; open violet downward triangle to $\overline{8}$S5 in the nematic phase; solid orange diamond to $\overline{8}$S5 in the SmA phase.

3. Results and discussion

Let us first consider the ECE measurements, which are shown in Figure 2. The data for tilt angle θ versus root mean square (rms) electric field E for the oxoesters LCV20158 and 9OO4 are shown for the SmA phase, both approximately 2°C below their respective nematic to SmA phase transition temperatures T_{NA}. A measurement of θ versus E in the nematic phase of these LCs was attempted, but the signal was too weak to be extracted from the noise. The resulting electroclinic coefficients are $e_c = (1.85 \pm 0.5) \times 10^{-13}$ and $(1.5 \pm 0.2) \times 10^{-13}$ rad m V^{-1} for LV20158 and 9OO4, respectively. These values of e_c should be compared to that of the thioester $\overline{8}$S5 in the SmA phase, where $e_c = (24.3 \pm 0.5) \times 10^{-13}$ rad m V^{-1}, which is more than an order of magnitude larger than for the oxoesters in the SmA phase; note that the companion thioester $\overline{7}$S5 does not have a SmA phase. In addition, we examined the two thioesters in the nematic phase, with the temperature of $\overline{8}$S5 approximately 2°C above T_{NA} and that of $\overline{7}$S5 approximately 2°C above the nematic–SmC transition temperature T_{NC}. In general, the ECE for a nematic phase of a chiral LC is considerably smaller than for the same material in the SmA phase [20]; the same holds true for mixtures of CNT + LC [17]. Nevertheless, we find that the values of e_c for the thioesters in the nematic phase are comparable to or even larger than the corresponding values of the oxoesters in the SmA phase, where $e_c =$
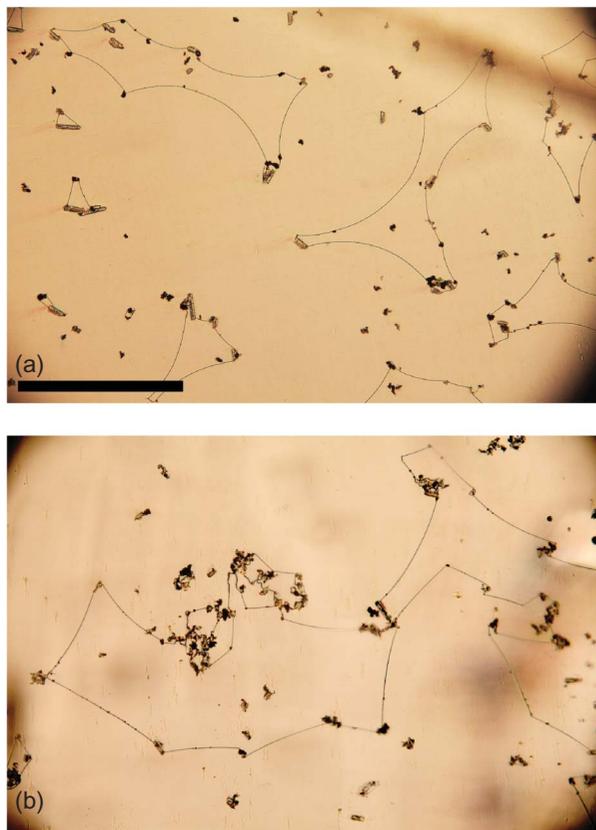
Figure 3. Curved disclination lines in the nematic phase demonstrating induced chirality in the liquid crystal in a planar 90° twist cell. The radius of curvature is proportional to the pitch *P*. (a) $\overline{7}S5$ and (b) 9OO4. The solid bar represents 250 μm.

$(2.37 \pm 0.12) \times 10^{-13}$ rad m V^{-1} for $\overline{8}S5$ and $(5.14 \pm 0.2) \times 10^{-13}$ rad m V^{-1} for $\overline{7}S5$. (That e_c for $\overline{7}S5$ is somewhat larger than for $\overline{8}S5$ reflects the fact that the measurements in $\overline{7}S5$ were performed in the nematic phase but close to the SmC phase transition temperature, where the tilt susceptibility is expected to be large.) The results in Figure 2, especially those comparing the thioester $\overline{8}S5$ with the two oxoesters in the same (SmA) phase, suggest that the chiral induction is considerably stronger in the thioester. To be sure, the ECE also depends strongly on the magnitude and location of the transverse dipole moment. For all of the materials, however, the main contribution to the dipole is expected to come from the carbonyl group in the central linkage. The presence of the two fluorines in the difluorophenyl benzoate LCV20158 seems to make very little difference in the ECE, at least compared to 9OO4. Thus, although there may be some differences in the transverse dipole moments among the three species (LCV20158, 9OO4 and $\overline{8}S5$) having a SmA phase, these are not expected to be significant, at least not compared to the more than one

order of magnitude difference between the electroclinic coefficients of $\overline{8}S5$ and of the oxoesters.

Turning to the pitch measurements in Figure 3, we extracted the inverse pitch P^{-1} from the radii of curvature R using the formula $P = 2R$ [27]. Because the CNT concentration is small and not uniform, there is a variation of the radius of curvature over the image [18]. Thus, we fitted each image along eight different arc segments to obtain an average pitch and variation. For the oxoester 9OO4 we obtained an inverse pitch $P^{-1} = (4.8 \pm 0.9) \times 10^{-4}$ μm^{-1} and for the thioester an inverse pitch $P^{-1} = (21 \pm 2) \times 10^{-4}$ μm^{-1}. Thus, the measured inverse pitch of the thioester sample is 4.4 ± 0.9 times larger than that of the oxoester. However, the CNT concentration of the thioester was smaller by a factor of 0.83. Correcting for the concentration difference, we find that the actual twisting power of the CNTs in the thioester is larger than that in the oxoester by a factor of 5.3 ± 0.9. It must be kept in mind that the helical pitch is not as strongly sensitive to the transverse dipole moment as is the ECE. Moreover, the elastic constants from one LC to another differ by factors much smaller than this ratio of 5.3 [29]. Thus, the clear message that emerges from the combined ECE and pitch data is that chirality can be induced by a chiral CNT in an achiral thioester LC much more readily than in an oxoester. We note that this trend in twist induction is not limited to CNT-induced chirality: we also examined the induced pitches for the commercial chiral dopant CB15 (Merck) and the chiral binaphthyl dopant 2,2'-dimethoxy-1,1'-binaphthyl, each in both 9OO4 and $\overline{7}S5$. The same quantitative trends, that is, much stronger chirality induced in the thioester LC, were observed [30].

Finally, let us address two issues regarding the nanotubes. As best as we can tell from these measurements, and also based upon previous results [16–18], the sign of the chirality remains the same in every experiment using CNTs from the batch supplied by the manufacturer. This suggests that the sign of the chirality likely is due to a systematic effect in the production method, although we cannot completely exclude the much less likely possibility of chiral segregation during manufacturing and subsequent removal of an aliquot having a nonzero enantiomer excess. Secondly, we note that we have examined single-walled nanotubes from another source, finding minimal chirality transfer [30]. We have not yet determined whether the near absence of chirality transfer is due to a much smaller *ee* in our sample of single-walled than in the multi-walled CNTs, or whether the much smaller radius of curvature of the single-walled CNTs is responsible for the reduced chirality transfer. This will be a topic of future investigation.

How do we explain these results? Conformational analyses of the model compounds phenyl benzoate and thiophenyl benzoate carried out at the B3LYP/6-31G* level for rotation about the Ph–O and Ph–S bonds, respectively, suggest that both cores adopt a chiral conformation in the ground state, as shown in Figure 4. The dihedral angle formed by the atoms C(O), X, C-1 and C-2 in the ground state conformer is 48° for X = O and 64° for X = S. It is generally accepted that chirality transfer in such a LC is achieved by chiral conformational interactions between a chiral dopant and the 'dynamically racemic' LC that can shift its equilibrium between left- and right-handed chiral conformers to produce a statistically larger population of chiral conformers of one handedness [1, 2]. The strength of the resulting chiral perturbation and its persistence length in the mesophase should be functions of a number of factors, including the height of the rotational barrier between chiral conformers and the dihedral angle corresponding to the helicity of the chiral conformation. As shown in Figure 4, the conformational analysis suggests that the rotational barrier in the gas phase for both model compounds is quite low, and is actually higher for the oxoester (0.4 kcal mol^{-1}) than for the thioester (0.2 kcal mol^{-1}), which is apparently inconsistent with ECE and pitch results. On the other hand, the chiral topography of the ground state conformer of the thiophenyl benzoate core, as shown by the dihedral angle formed by C(O), X, C-1 and C-2, is more pronounced than that of the phenyl benzoate core, as shown in Figure 5.

Another key factor to consider in understanding the difference in ECE and inverse pitch induced by the
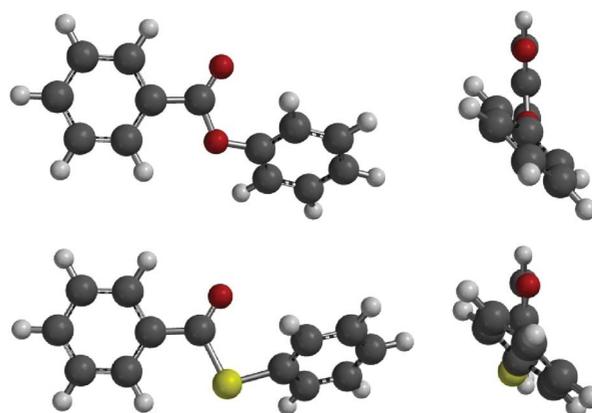
Figure 5. Side-on and end-on views of the lowest energy conformers of phenyl benzoate (top) and thiophenyl benzoate (bottom) according to B3LYP/6-31G* calculations.

CNT in oxoester and thioester hosts is the strength of the non-covalent interactions between the CNT and the host molecules that gives rise to chirality transfer [1, 2]. For example, Williams and Lemieux [31] previously showed in helical twisting power (HTP) measurements of axially chiral biphenyl dopants that the HTP in the nematic host 5CB increases with substituents of increasing polarisability, which is consistent with an increase in dispersive forces between dopant and hosts. In the present case, the nature of the interaction between the CNT and LC host that gives rise to chirality transfer remains unclear, but it likely depends on the strength of non-covalent interactions between the two materials, which should be primarily dispersive in nature. Hence, one should expect such interactions to be stronger between the CNT and thiophenyl benzoate hosts, given the higher polarisability of sulfur compared to that of oxygen. We suggest that this stronger non-covalent interaction associated with the thioester compounds is another important factor contributing to the larger electroclinic response and macroscopic inverse helical pitch.

We remark that the chiral signatures also may be due in part to an indirect chiral coupling to the CNTs. Because the chiral wrapping of the CNTs results in a tilt of the director at the CNT wall relative to the CNT axis [32] and the condition that the director becomes parallel to the CNT axis far from the wall, the nematic director must undergo a twist in the vicinity of the CNT. The elastic energy cost of this imposed macroscopic mechanical twist may be offset partially by inducing a small conformational enantiomeric excess in the otherwise achiral LC. This work will be reported elsewhere [33].
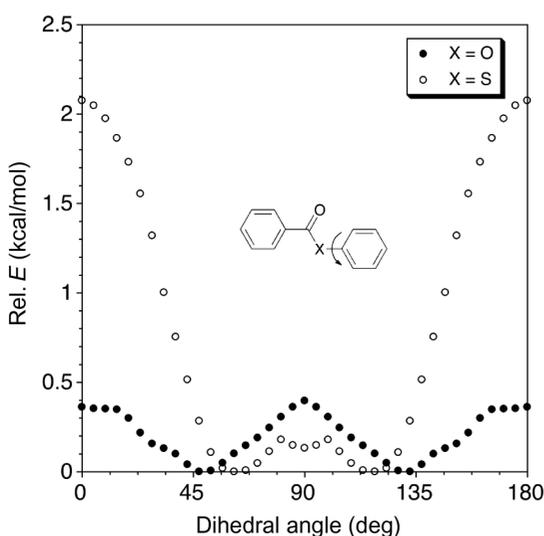

Figure 4. Energy profile for phenyl benzoate (X = O) and thiophenyl benzoate (X = S) as a function of the dihedral angle defined by C(O), X, C-1 and C-2 according to B3LYP/6-31G* calculations.

4. Conclusions

We have shown that chiral dopants, particularly a dispersion of multi-walled CNTs having a non-zero

enantiomeric excess, can induce chirality into the suspending liquid crystalline matrix. The chiral signatures of an ECE and a macroscopic helical twist of the director were found to be much stronger for mesogens containing a thioester linkage than those containing an oxoesters linkage. Although conformational energy calculations in the gas phase suggest an extremely weak chiral preference for the oxoesters, we suggest that the much stronger chiral susceptibility of the thioester is due to its higher polarisability, thus resulting in stronger non-covalent interactions with the chiral dopant.

Acknowledgements

References

[1] Pieraccini, S; Ferrarini, A.; Spada, G.P. *Chirality* **2008**, *20*, 749–759.
[2] Pieraccini, S.; Masiero, S.; Ferrarini, A.; Spada, G.P. *Chem. Soc. Rev.* **2011**, *40*, 258–271.
[3] Eelkema, R.; Feringa, B.L. *Org. Biomol. Chem.* **2006**, *4*, 3729–3745.
[4] Amabilino, D.B.; Veciana, J. *Top. Curr. Chem.* **2006**, *265*, 253–302.
[5] Lemieux, R.P. *Acc. Chem. Res.* **2001**, *34*, 845–853; Lemieux, R.P. *Chem. Soc. Rev.* **2007**, *36*, 2033–2045.
[6] Baik, In-Su; Jeon, S.Y.; Lee, S.H.; Park, K.A.; Jeong, S.H.; An, K.H.; Lee, Y.H. *Appl. Phys. Lett.* **2005**, *87*, 263110. DOI:10.1063/1.2158509
[7] Park, K.A.; Lee, S.M.; Lee, S.H.; Lee, Y.H. *J. Phys. Chem. C* **2007**, *111*, 1620–1624.
[8] Lynch, M.D.; Patrick, D.L. *Nano Lett.* **2002**, *2*, 1197–1201.
[9] Dierking, I.; Scalia, G.; Morales, P. *J. Appl. Phys.* **2005**, *97*, 044309. DOI:10.1063/1.1850606
[10] Basu, R.; Iannacchione, G. *Appl. Phys. Lett.* **2008**, *93*, 183105. DOI:10.1063/1.3005590
[11] Dierking, I.; Scalia, G.; Morales, P.; LeClere, D. *Adv. Mater.* **2004**, *16*, 865–869.
[12] Lagerwall, J.P.F.; Scalia, G. *J. Mater. Chem.* **2008**, *18*, 2890–2898.
[13] van der Schoot, P.P.A.M.; Popa-nita, V.; Kralj, S. *J. Phys. Chem. B* **2008**, *112*, 4512–4518.
[14] Basu, R.; Iannacchione, G. *Appl. Phys. Lett.* **2009**, *95*, 173113. DOI:10.1063/1.3256013
[15] Basu, R.; Iannacchione, G. *Phys. Rev. E: Stat., Nonlinear, Soft Matter Phys.* **2010**, *81*, 051705. DOI:10.1103/PhysRevE.81.051705
[16] Basu, R.; Boccuzzi, K.A.; Ferjani, S.; Rosenblatt, C. *Appl. Phys. Lett.* **2010**, *97*, 121908. DOI:10.1063/1.3492844
[17] Basu, R.; Petschek, R.G.; Rosenblatt, C. *Phys. Rev. E: Stat., Nonlinear, Soft Matter Phys.* **2011**, *83*, 041707. DOI:10.1103/PhysRevE.83.041707
[18] Basu, R.; Chen, C.-L.; Rosenblatt, C. *J. Appl. Phys.* **2011**, *109*, 083518. DOI:10.1063/1.3576101
[19] Garoff, S.; Meyer, R.B. *Phys. Rev. Lett.* **1977**, *38*, 848–851.
[20] Li, Z.; Petschek, R.G.; Rosenblatt, C. *Phys. Rev. Lett.* **1989**, *62*, 796–799.
[21] Li, Z.; DiLisi, G.A.; Petschek, R.G.; Rosenblatt, C. *Phys. Rev. A: At., Mol., Opt. Phys.* **1990**, *41*, 1997–2004.
[22] Li, Z.; Ambigapathy, R.; Petschek, R.G.; Rosenblatt, C. *Phys. Rev. A: At., Mol., Opt. Phys.* **1991**, *43*, 7109–7112.
[23] Etxebarria, J.; Zubia, J. *Phys. Rev. A: At., Mol., Opt. Phys.* **1991**, *44*, 6626–6631.
[24] Shao, R.F.; Maclennan, J.E.; Clark, N.A.; Dyer, D.J.; Walba, D.M. *Liq. Cryst.* **2001**, *28*, 117–123.
[25] Ferjani, S.; Choi, Y.; Pendery, J.; Petschek, R.G.; Rosenblatt, C. *Phys. Rev. Lett.* **2010**, *104*, 257801. DOI:10.1103/PhysRevLett.104.257801
[26] Berardi, R.; Kuball, H.-G.; Memmer, R.; Zannoni, C. *J. Chem. Soc., Faraday Trans.* **1998**, *94*, 1229–1234.
[27] Raynes, E.P. *Liq. Cryst.* **2006**, *33*, 1215–1218.
[28] Andersson, G.; Dahl, I.; Keller, P.; Kuczynski, W.; Lagerwall, S.T.; Skarp, K.; Stebler, B. *Appl. Phys. Lett.* **1987**, *51*, 640–642.
[29] DeGennes, P.G.; Prost, J. *The Physics of Liquid Crystals*; Clarendon: Oxford, 2004.
[30] Basu, R.; Rosenblatt, C.; Lemieux, R.P.; unpublished.
[31] Williams, V.E.; Lemieux, R.P. *Chem. Commun.* **1996**, 2259–2260.
[32] Iijima, S. *Nature* **1991**, *354*, 56–58.
[33] Basu, R.; Pendery, J.; Rosenblatt, C.; Lemieux, R.P. to be published.